ANNALS OF THE UNIVERSITY OF CRAIOVA
ANNALES DE L'UNIVERSITÉ DE CRAIOVA

ANALELE UNIVERSITĂȚII DIN CRAIOVA

SERIA: INGINERIE ELECTRICĂ
SERIE: ELECTRICAL ENGINEERING
SÉRIE: INGÉNIERIE ÉLECTRIQUE
Anul/Year/Année 37
No. 37, 2013

EDITURA UNIVERSITARIA

ANNALS OF THE UNIVERSITY OF CRAIOVA
ANNALES DE L'UNIVERSITÉ DE CRAIOVA

ANALELE UNIVERSITĂȚII DIN CRAIOVA

SERIA: INGINERIE ELECTRICĂ
SERIE: ELECTRICAL ENGINEERING
SÉRIE: INGÉNIERIE ÉLECTRIQUE
Anul/Year/Année 37
No. 37, 2013

ISSN 1842 - 4805

EDITURA UNIVERSITARIA

ANNALS OF THE UNIVERSITY OF CRAIOVA

A. I. Cuza str., no. 13
ROMANIA

We exchange publications with similar institutions of country and from abroad

ANNALES DE L'UNIVERSITÉ DE CRAIOVA

13, rue A. I. Cuza
ROUMANIE

On fait des échanges des publications avec les institutions similaires du pays et de l'étranger

This journal is published by the Faculty of Electrical Engineering from the University of Craiova.

This issue contains mainly papers selected from the 9th International Conference on Electromechanical and Power Systems – SIELMEN 2013, October 15-16, 2013, Iaşi, România; October 17-18, 2013, Chişinău, Moldova.

UNIVERSITY OF CRAIOVA

FACULTY OF ELECTRICAL ENGINEERING

INTERNATIONAL SCIENTIFIC COMMITTEE

Maricel ADAM	*"Gh. Asachi" Technical University of Iasi*	Romania
Mihaela ALBU	*University Politehnica of Bucharest*	Romania
Slavoljub ALEKSIC	*University of Nis*	Serbia
Horia BALAN	*Technical University of Cluj-Napoca*	Romania
Maria BROJBOIU	*University of Craiova*	Romania
Aurel CAMPEANU	*University of Craiova*	Romania
Mihai CERNAT	*Transilvania University of Brasov*	Romania
Marian CIONTU	*University of Craiova*	Romania
Grigore CIVIDJIAN	*University of Craiova*	Romania
Zlata CVETCOVIC	*University of Nis*	Serbia
Daniela DANCIU	*University of Craiova*	Romania
Sonia DEGERATU	*University of Craiova*	Romania
Iuliu DELEŞEGA	*University Politehnica of Timisoara*	Romania
Silvia-Maria DIGĂ	*University of Craiova*	Romania
Peter DINEFF	*Technical University of Sofia*	Bulgaria
Radu DOBRESCU	*University Politehnica of Bucharest*	Romania
Radu DOBRESCU	*University Politehnica of Bucharest*	Romania
Sorin ENACHE	*University of Craiova*	Romania
Virgiliu FIREȚEANU	*University Politehnica of Bucharest*	Romania
Dan FLORICAU	*University Politehnica of Bucharest*	Romania
Stefan HARAGUS	*University Politehnica of Timisoara*	Romania
Elena HELEREA	*Transilvania University of Brasov*	Romania
Eugen HNATIUC	*"Gh. Asachi" Technical University of Iasi*	Romania
Kemal HOT	*Polytechnic of Zagreb*	Croatia
Nathan IDA	*University of Akron*	USA
Maria IOANNIDES	*National Technical University of Athens*	Greece
Valentin IONITA	*University Politehnica of Bucharest*	Romania
Mihai IORDACHE	*University Politehnica of Bucharest*	Romania
Sergiu IVANOV	*University of Craiova*	Romania
Wilhelm KAPPEL	*National Research and Development Institute for Electrical Engineering (ICPE – CA) Bucharest*	Romania
Lucian MANDACHE	*University of Craiova*	Romania
Leonardo-Geo MĂNESCU	*University of Craiova*	Romania
Gheorghe MANOLEA	*University of Craiova*	Romania
Andrei MARINESCU	*Research, Development and Testing National Institute for Electrical Engineering Craiova (ICMET)*	Romania
Iliana MARINOVA	*Technical University of Sofia*	Bulgaria
Ernest MATAGNE	*Université Catholique de Louvain*	Belgium
Dan MIHAI	*University of Craiova*	Romania
Alexandru MOREGA	*University Politehnica of Bucharest*	Romania
Mihaela MOREGA	*University Politehnica of Bucharest*	Romania
Nazih MOUBAYED	*Lebanese University*	Lebanon
Călin MUNTEANU	*Technical University of Cluj-Napoca*	Romania

Florin MUNTEANU	*"Gh. Asachi" Technical University of Iasi*	Romania
Valentin NĂVRĂPESCU	*University Politehnica of Bucharest*	Romania
Petre-Marian NICOLAE	*University of Craiova*	Romania
Petru NOTINGHER	*University Politehnica of Bucharest*	Romania
Vasile NUȚU	*Military Technical Academy*	Romania
Ioan POPA	*University of Craiova*	Romania
Mihaela POPESCU	*University of Craiova*	Romania
Miroslav PRSA	*University of Novi-Sad*	Serbia
Mircea M. RADULESCU	*Technical University of Cluj Napoca*	Romania
Benoit ROBYNS	*Ecole des Hautes Etude d'Ingénieur de Lille*	France
Constantin ROTARU	*Military Technical Academy*	Romania
Alex RUDERMAN	*Elmo Motion Control Ltd*	USA
Sergey RYVKIN	*Trapeznikov Institute of Control Sciences*	Russia
Constantin SARMASANU	*"Gh. Asachi" Technical University of Iasi*	Romania
Dan SELIŞTEANU	*University of Craiova*	Romania
Victor SONTEA	*Technical University of Moldova*	Moldova
Alexandru STANCU	*"A.I. Cuza" University of Iaşi*	Romania
Viorel STOIAN	*University of Craiova*	Romania
Ryszard STRZELECKI	*University of Technology Gdansk*	Poland
Flavius-Dan SURIANU	*University Politehnica of Timisoara*	Romania
Raina TZENEVA	*Technical University of Sofia*	Bulgaria
Ioan VĂDAN	*Technical University of Cluj-Napoca*	Romania
Viorel VARVARA	*"Gh. Asachi" Technical University of Iasi*	Romania
Ion VLAD	*University of Craiova*	Romania

Dynamic Performance Analysis of Deep Bars Squirrel Cage Induction Motor by Simulation

Mihai Iordache*, Lucia Dumitriu*, Dragos Niculae*, Neculai Galan*, Sorin Deleanu† and Lucian Mandache**
* "Politehnica" University of Bucharest, Romania, mihai.iordache@upb.ro, lucia.dumitriu@upb.ro, dragos.niculae@upb.ro, galannicolae@yahoo.com
† Northern Alberta Institute of Technology, Edmonton, Canada, sorind@nait.ca
** University of Craiova, Faculty of Electrical Engineering, Craiova, Romania, lmandache@elth.ucv.ro

Abstract - **The rotor parameters of the squirrel cage induction machine, resistance and leakage inductance, depend upon the frequency of the rotor circuit, mostly due to the skin effect. For low values of the rotor frequency (less than 10 - 15 Hz), corresponding to the quasi-linear branch of the torque-speed curve between synchronous speed and the critical one, the skin effect is quite insignificant. However, for higher frequencies (e.g. 50Hz and/or 60Hz, at starting), this variation of the parameters cannot be neglected. In this paper, the analytic relationships developed for expressing the rotor resistance and leakage inductance as functions of slip/frequency, directly result from the skin effect theory. The induction motor model based upon Park-Blondel equations have been used to analyze its dynamic (transient) behavior. Park-Blondel equations are nonlinear, because of their intrinsic structure, the rotor parameters variation with the frequency, saturation of the magnetic core, and the dependency of the load torque with respect to the rotor angular frequency. For solving the induction motor system of equations, the authors used MATLAB software package due to its enhanced capabilities in terms of integrating ordinary differential equations. When analyzing the induction motor operating at steady state, we used the well-known Ő (Steinmetz) per-phase equivalent circuit. Although, the magnetizing inductance is considered as the current-controlled nonlinear inductor while the rotor resistor as a time-variable resistor. For steady-state analysis, both ENCAP (Electrical Nonlinear Circuit Analysis) and SPICE software packages have been used in order to be able to assess the results. In both cases, the induction motor model is derived from modified nodal equations. This gives the possibility to apply Fourier analysis for all current and voltage waveforms and compute any high order harmonics. Following the computing of harmonic content, we assessed the steady state characteristics (power factor, efficiency, etc.) of the induction motor, while the equivalent circuit parameters determined through calculations closely match the parameter values obtained from the catalogue data.**

Keywords - *induction motor, state equations, transient behavior, deep rotor bars, saturation phenomena, stead-steady behavior, skin effect*

I. INTRODUCTION

In many studies regarding the estimation the induction machine parameters, the authors included the skin effect and the saturation of the magnetic circuit [1-9, 12-14]. When considering applications of electric AC drives using three-phase induction motors with deep bars in the rotor circuit, both mathematical model of the induction motor and the overall control strategy have been modified in order to maximize the performance [6]. Most of the vector drives use to rotor flux control due to the simplicity of the mathematical model which demands less "real-time" computation.

However, for the motor with deep rotor bars, the rotor flux significantly varies inside the rotor magnetic core, so cannot be precisely defined. As a result, the drive control using the air gap flux appears as an attractive alternative. However, when using the pseudo rotor flux, one can achieve similar performances to the rotor flux orientation case, when considering the equivalent rotor parameters. The squirrel cage with deep rotor bars can be made equivalent with a two rotor cages, one of these described by constant parameters [8].

The induction motor with deep bars is described by a mathematical model which includes the skin effect upon the rotor parameters and the saturation of the magnetic circuit as well and enables the simulation of various operating modes. The frequency of the stator winding is constant and equal to the power supply frequency, resulting constant stator parameters. The rotor parameters are assumed constant, independent of the rotor current frequency when this one has low values (0 to 10…15 Hz, the latter one usually being associated with the critical slip/speed). However, for higher values of the rotor current frequency, the rotor resistance and leakage inductance depend upon the frequency (slip) through relationships developed from the skin effect theory.

In addition to the skin effect, the saturation of the magnetic circuit comes into effect when the magnetizing inductivity L_m varies. In Fig. 1, L_m appears variable in time. In fact, this curve explains the magnetic circuit saturation effect during the start-up process, when the induction motor has deep bars. In order to approach real starting condition, a load torque M_r, variable with the speed was proposed in Fig. 2.

The induction motor analysis for steady-state analysis purpose requires the state equations referred to the "*d*, *q*, 0" system of coordinates, in which the time derivatives are made equal to zero, excepting the mechanical equation. Once integrated over a long time span, the mechanical equation can deliver the steady state value of rotor mechanical speed and consequently, the stator and rotor currents, electromagnetic torque, etc.

Other methods for obtaining the steady state characteristics are based upon the solving of the induction motor equivalent circuit (see Fig. 3) or by applying the state equations and / or the modified nodal equations.

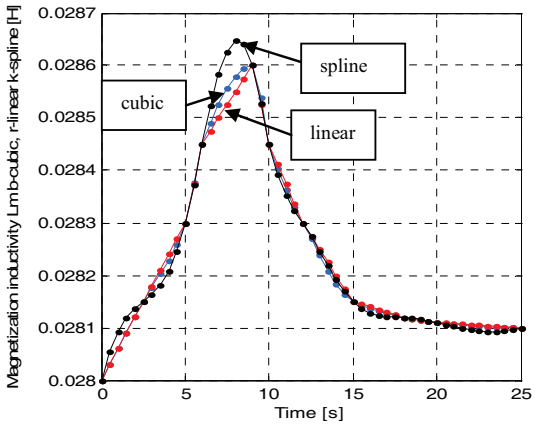

Fig. 1. The magnetization inductivity variation versus time.

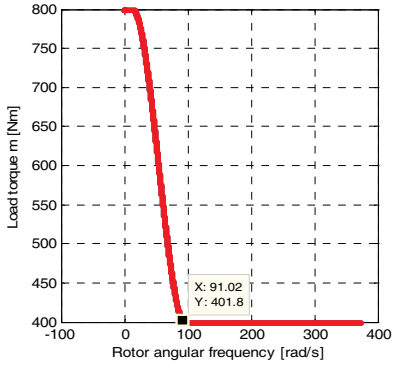

Fig. 2. The load torque variation versus rotor angular frequency.

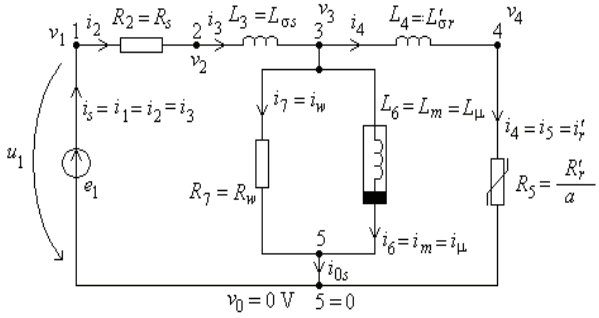

Fig. 3. Induction motor equivalent circuit.

The latter one (called the *brute force*) involves a number of iterations until the steady state solutions is obtained, through a process which must satisfy an imposed convergence criterion [10, 11, 14].

The first major outcome of this paper was to analyze the deep bars induction motor steady state behavior and characteristics for non-saturated magnetic circuit versus the situation when we assumed the magnetic circuit saturated (see the $\prod$ equivalent circuit of the induction motor shown in Fig. 3). When the magnetic circuit saturation was included, the magnetization inductor $L_6 = L_m$ was modeled as a current-controlled nonlinear inductor with its magnetic flux depending upon the magnetizing current $\varphi = \hat{\varphi}(i_m)$. However, in this paper, the steady state study follows the transient study as particular regime.

The second major outcome of this paper was to analyze the transient behavior of the deep bars induction motor, using the state equations and/or the modified nodal equations in the time domain (the semi-state equations), based on the brute force method. For transient purposes, the rotor resistor R'_r/a (a – being the slip) was modeled as a time-variable (parametric) function, in which the slip was calculated at each time step.

The simulations were performed by using the SPICE and/or the ENCAP – Electrical Nonlinear Circuit Analysis software packages [10, 11]. When using these packages, the deep bars induction motor model was constructed in terms of the modified nodal equations, being very appropriate for the Fourier analysis for all current and voltage waveforms. In this way we could compute any high order voltage/current harmonics, following the determination of the time dependency of such quantities. The voltage/current harmonic calculation represents the input towards the deep bars induction motor performances assessment (e.g. more harmonic content means less efficiency, poor power factor, etc.).

In addition to the performances, some adjacent effects like the electromagnetic forces and the parasitic torques can be analytically approximated from voltage/current harmonics [15].

II. Simulation of the Induction Motor for Transient Conditions

The induction motor transient analysis was performed starting with the dynamic state equations expressed in the d, q, 0 reference frame and the rotor quantities referred to the stator [7]:

$$\frac{d\varphi_{sd}}{dt} = -R_s\left(\frac{1}{\sigma L_s}\left(\varphi_{sd} - \frac{L_m}{L'_r}\varphi'_{rd}\right)\right) + \omega_1\varphi_{sq} + u_{sd} \quad (1,a)$$

$$\frac{d\varphi_{sq}}{dt} = -R_s\left(\frac{1}{\sigma L_s}\left(\varphi_{sq} - \frac{L_m}{L'_r}\varphi'_{rq}\right)\right) - \omega_1\varphi_{sd} + u_{sq} \quad (1,b)$$

$$\frac{d\varphi'_{rd}}{dt} = -R'_r\left(\frac{1}{\sigma L'_r}\left(\varphi'_{rd} - \frac{L_m}{L_s}\varphi_{sd}\right)\right) + (\omega_1 - \omega)\varphi'_{rq} \quad (1,c)$$

$$\frac{d\varphi'_{rq}}{dt} = -R'_r\left(\frac{1}{\sigma L'_r}\left(\varphi'_{rq} - \frac{L_m}{L_s}\varphi_{sq}\right)\right) - (\omega_1 - \omega)\varphi'_{ra} \quad (1,d)$$

$$\frac{d\omega}{dt} = \frac{3p^2}{2J}\left(\varphi_{sd}\frac{1}{\sigma L_s}\left(\varphi_{sq} - \frac{L_m}{L'_r}\varphi'_{rq}\right) - \varphi_{sq}\frac{1}{\sigma L_s}\left(\varphi_{sd} - \frac{L_m}{L'_r}\varphi'_{rd}\right)\right) - \frac{pM_r}{J} \quad (1,e)$$

$$\frac{d\theta}{dt} = \omega \quad (1,f)$$

where: φ_{sd} - is the stator magnetic flux axis in the direction of "d-axis", φ_{sq} - represents the stator magnetic flux in the direction of "q-axis" (quadrature), φ'_{rd} - is the rotor magnetic flux along the "d-axis", φ'_{rq} - represents the

rotor magnetic flux with respect to the "q-axis", ω – is the rotor angular frequency ($\omega = p\Omega$, p – number of the pole pairs and Ω is the mechanical angular speed), $\omega_r = \omega_1 - \omega$ - is the rotor current angular frequency, ω_1 - represents the stator angular frequency and θ - is the electric angle which gives the rotor position in respect of the stator (see Fig. 4, θ is the angle between the FS axis and FR axis). In the majority of the models FS designates the magnetic axis of stator "phase A" winding while the FR stays for the rotor "phase a" winding.

The state vector has the following expression:

$$\boldsymbol{x} = \left[\varphi_{sd}, \varphi_{sq}, \varphi'_{rd}, \varphi'_{rq}, \omega, \theta\right]^{t}. \tag{2}$$

The stator and the rotor magnetic fluxes can be expresses as functions of the currents and inductances as following:

$$\begin{aligned} \varphi_{sd} &= L_s i_{sd} + L_m i'_{rd}; \qquad \varphi_{sq} = L_s i_{sq} + L_m i'_{rq}; \\ \varphi'_{rd} &= L'_r i'_{rd} + L_m i_{sd}; \qquad \varphi'_{rq} = L'_r i'_{rq} + L_m i_{sq}. \end{aligned} \tag{3}$$

When solving the equations (3) for the currents i_{sd}, i_{sq}, i'_{rd} and i'_{rq} we obtained:

$$\begin{aligned} i_{sd} &= \frac{1}{\sigma L_s}\left(\varphi_{sd} - \frac{L_m}{L'_r}\varphi'_{rd}\right), i_{sq} = \frac{1}{\sigma L_s}\left(\varphi_{sq} - \frac{L_m}{L'_r}\varphi'_{rq}\right), \\ i'_{rd} &= \frac{1}{\sigma L'_r}\left(\varphi'_{rd} - \frac{L_m}{L_s}\varphi_{sd}\right), i'_{rq} = \frac{1}{\sigma L'_r}\left(\varphi'_{rq} - \frac{L_m}{L_s}\varphi_{sq}\right). \end{aligned} \tag{4}$$

In the relations (1) – (4) have been used the: $u_{sd} = \sqrt{2}U_1$; $u_{sq} = 0.0$; R_s – is the stator resistance; R'_r – represents the rotor resistance referred to the stator; L_s – is the cyclical stator inductance, defined as the sum of the stator leakage inductance $L_{s\sigma}$ and the useful cyclical stator inductance L_{11}; L'_r – represents the cyclical rotor inductance, defined as the sum between the rotor leakage inductance $L'_{r\sigma}$ and the useful cyclical inductance L'_{22} - all of the rotor inductances are referred to the stator; L_m – is the cyclical mutual inductivity between the stator and the rotor, given by the relationship $L_m = 3M_m/2$, in which M_m is the maximum value of the mutual inductivity, measured between one stator phase winding and one rotor phase winding having the same direction; ω_1 - represents the stator angular frequency; ω - is the mechanical angular frequency (at the motor shaft); $\Omega_1 = \omega_1 / p$ - represents the angular speed of the revolving electromagnetic field with respect of the stator (synchronous speed); $\Omega = \omega / p$ - is the mechanical angular speed of the rotor; p – the number of the pole pairs; J – the rotor moment of inertia and M_r – is the load torque. The non-dimensional "leakage coefficient" σ has the expression:

$$\sigma = 1 - \frac{L_m^2}{L_s L'_r}. \tag{5}$$

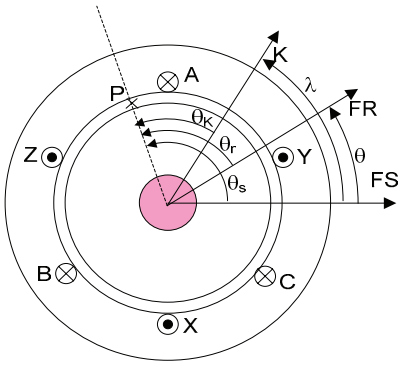

Fig. 4. Structure of the reference systems.

The electromagnetic torque can be calculated starting from the definition and using (4):

$$\begin{aligned} M &= \frac{3p}{2}\left(\varphi_{sd} i_{sq} - \varphi_{sq} i_{sd}\right) = \\ &= \frac{3p}{2}\left(\varphi_{sd} \cdot \frac{1}{\sigma L_s}\left(\varphi_{sq} - \frac{L_m}{L'_r}\varphi'_{rq}\right) - \right. \\ &\left. - \varphi_{sq} \cdot \frac{1}{\sigma L_s}\left(\varphi_{sd} - \frac{L_m}{L'_r}\varphi'_{rd}\right)\right) \end{aligned} \tag{6}$$

or:

$$\begin{aligned} M &= \frac{3p}{2}\left(\varphi'_{rd} i'_{rq} - \varphi'_{rq} i'_{rd}\right) = \\ &= \frac{3p}{2}\left(\varphi'_{rd} \frac{1}{\sigma L'_r}\left(\varphi'_{rq} - \frac{L_m}{L_s}\varphi_{sq}\right) - \right. \\ &\left. - \varphi'_{rq} \cdot \frac{1}{\sigma L'_r}\left(\varphi'_{rd} - \frac{L_m}{L_s}\varphi_{sd}\right)\right). \end{aligned} \tag{7}$$

The stator and rotor phase currents i_A, i_B, i_C respectively i'_a, i'_b, i'_c can by expressed, as function of the d, q, 0 stator and rotor currents following a transformation of coordinates [7]:

$$\begin{aligned} i_A(t) &= i_{ds}(t)\cdot\cos(\omega_1 t) - i_{qs}(t)\cdot\sin(\omega_1 t) + i_{0s}; \\ i_B(t) &= i_{ds}(t)\cdot\cos\left(\omega_1 t - \frac{2\pi}{3}\right) - i_{qs}(t)\cdot\sin\left(\omega_1 t - \frac{2\pi}{3}\right) + i_{0s}; \\ i_C(t) &= i_{ds}(t)\cdot\cos\left(\omega_1 t + \frac{2\pi}{3}\right) - i_{qs}(t)\cdot\sin\left(\omega_1 t + \frac{2\pi}{3}\right) + i_{0s}; \\ i'_a(t) &= i'_{dr}(t)\cdot\cos\left((\omega_1 - \omega)t\right) - i'_{qr}(t)\cdot\sin\left((\omega_1 - \omega)t\right) + i_{0r}; \\ i'_b(t) &= i'_{dr}(t)\cdot\cos\left((\omega_1 - \omega)t - \frac{2\pi}{3}\right) - i'_{qr}(t)\cdot\sin\left((\omega_1 - \omega)t - \frac{2\pi}{3}\right) + i_{0r}; \\ i'_c(t) &= i'_{dr}(t)\cdot\cos\left((\omega_1 - \omega)t + \frac{2\pi}{3}\right) - i'_{qr}(t)\cdot\sin\left((\omega_1 - \omega)t + \frac{2\pi}{3}\right) + i_{0r} \end{aligned} \tag{8}$$

Assuming the induction motor with identical phase windings characteristics, operating under balanced conditions, the stator and the rotor zero-sequence currents will not be present $i_{0s} = 0$, respectively $i_{0r} = 0$.

The skin effect analysis shows that the rotor resistance R'_r referred at the stator increases with $\sqrt{\omega_r}$, while the

leakage inductance $L'_{r\sigma}$ decreases with $\sqrt{\omega_r}$, where ω_r is the rotor angular frequency. Therefore, the rotor parameters referred to the stator can be expressed as following [7]:

$$\begin{aligned} &R'_r(\omega_r) = R'_r = ct. \quad \text{for } \omega_r \in (0, \omega_{rx}); \\ &R'_r(\omega_r) = k_1 + k_2\sqrt{\omega_r}; \ \omega_r > \omega_{rx}; \\ &L'_r(\omega_r) = L'_r = ct. \quad \text{for } \omega_r \in (0, \omega_{rx}); \\ &L'_r(\omega_r) = L_m + k_3 - \frac{k_4}{\sqrt{\omega_r}}; \ \omega_r > \omega_{rx}. \end{aligned} \tag{9}$$

The constants k_1, k_2, k_3 and k_4 are determined from the continuity condition at the point $\omega_r = \omega_{rx}$ (ω_{rx} represents the value of the angular frequency associated with the critical slip), while the values of the electrical parameters for the squirrel cage at starting point (slip value $a = 1$), can be extracted from the available catalogue data for an induction motor.

Typically for the range $\omega_r < \omega_{rx}$, the rotor parameters are considered constant, while for $\omega_r \geq \omega_{rx}$ the rotor parameters vary with the rotor angular frequency ω_r according to relations (9). These are valid for a wide range of frequencies from rotor circuit.

As example, we consider an induction motor for designated for traction purposes (MABT-2). This induction motor has the following ratings:

$P_n = 100$ kW; $U_n = 560$ V; $U_{fn} = 323.32$ V; $I_{fn} = I_n = 130$ A; $n_1 = 1200$ rpm, $n = 1168.8$ rpm - n_1 (n) is the synchronous revolving speed; $Z_b = Z_n = U_{fn}/I_{fn} = 2.48\ \Omega$; $f_n = f_1 = 60$ Hz; $p = 3$; $R_s = 0.053\ \Omega$; $R'_r = 0.0657\ \Omega$; $L_{s\sigma} = 1.034$ mH; $L'_{r\sigma} = 0.955$ mH; $L_m = 28.1$ mH; $\eta = 0.897$ %; $\cos\varphi_{1n} = 0.87$; $J = 3.38$ kgm^2 or $J = 60.0$ kgm^2; $i_p = \frac{I_{fp}}{I_{fn}} = 4$; $m_p = \frac{M_p}{M_n} = 1.1$; $m_m = \frac{M_m}{M_n} = 1.8$. Stator windings have a Y-connection.

With the values from above, the next quantities are calculated: $M_n = 817$ Nm; $M_p = 898.7$ Nm; $I_p = 520$ A; $S_n = 128094.8$ VA; $a_n = 0.026$; $P_{1n} = S_n \bullet \cos\varphi_{1n} = 111442.5$ W.

From [7], if $\omega_{rx} = 81$ rad/s, when introducing the data from above in the relationships (9), the numerical values for the rotor electrical parameters referred to the stator can be described as:

$$\begin{aligned} &L'_r(\omega_r) = 0{,}0281 + \begin{cases} 0{,}000955\,H; & \omega_r \in [0; 81] \\ 0{,}000155 + 0{,}0072\dfrac{1}{\sqrt{\omega_r}}; & 81 < \omega_r \leq \omega_1 \end{cases} \\ &R'_r(\omega_r) = \begin{cases} 0{,}065434; & \omega_r \in [0; 81] \\ 0.000904 + 0{,}00717\sqrt{\omega_r}; & 81 < \omega_r \leq \omega_1 \end{cases} \\ &\text{with} \quad \omega_1 = 120\pi \end{aligned} \tag{10}$$

A complete procedure for determining the transient behavior at starting of the squirrel cage induction motor with deep bars consists of the following steps:

• In the dynamic state equations (1), the rotor electrical parameters are introduced using the relationships (10), which in fact consider the skin effect.

• The influence of the magnetic circuit saturation is revealed by the dependency of the magnetic inductance with the time given in Fig. 1.

The load torque encountered by the induction motor at the shaft has a time dependency given in Fig. 2.

Following the application of some ordinary integration routines (available in MATLAB programming environment) to solve the equations (1), we've obtained the results summarized in Fig. 5 – 18.

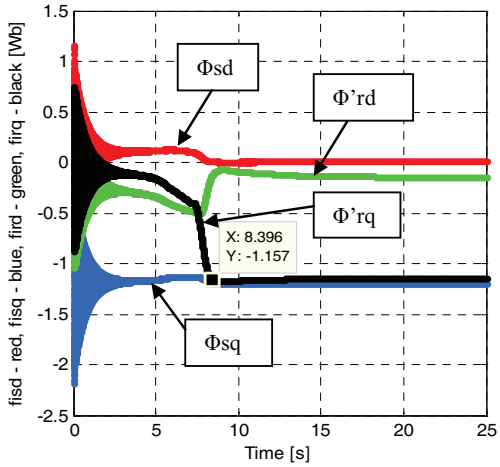

Fig. 5. The stator and rotor magnetic fluxes in the d, q, 0 reference frame as functions of time.

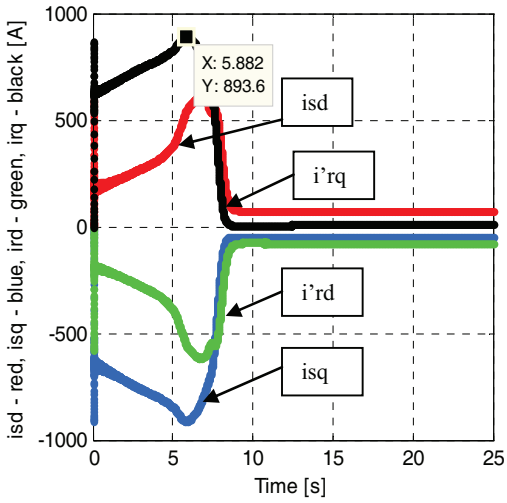

Fig. 6. The stator and rotor currents in the d, q, 0 reference frame as functions of time.

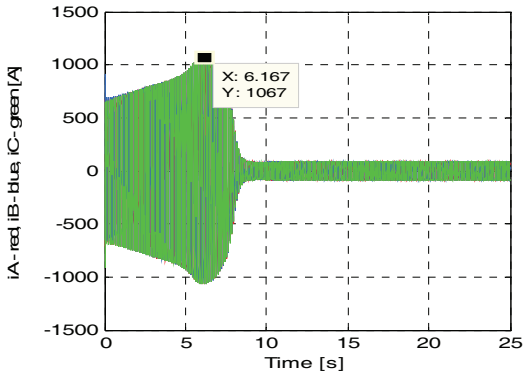

Fig. 7. The stator currents as functions of time.